Observation of In-Band Lattice Solitons

Xiaosheng Wang[1] and Zhigang Chen[1,2]
[1]Department of Physics and Astronomy, San Francisco State University, San Francisco, California 94132, USA
[2]TEDA Applied Physical School, Nankai University, Tianjin 300457, China

Jiandong Wang and Jianke Yang
Department of Mathematics and Statistics, University of Vermont, Burlington, Vermont 05401, USA
(Received 4 August 2007; published 14 December 2007)

We report the first experimental and theoretical demonstrations of in-band (or embedded) lattice solitons. Such solitons appear in trains, and their propagation constants reside *inside* the first Bloch band of a square lattice, different from all previously observed solitons. We show that these solitons bifurcate from Bloch modes at the interior high-symmetry X points within the first band, where normal and anomalous diffractions coexist along two orthogonal directions. At high powers, the in-band soliton can move into the first band gap and turn into a gap soliton.

DOI: 10.1103/PhysRevLett.99.243901 PACS numbers: 42.65.Tg, 42.65.Sf, 42.65.Wi, 42.82.Et

Solitons are nonlinear wave phenomena ubiquitous in nature [1], from fluid dynamics to biological systems, and from nonlinear optics to Bose-Einstein condensates (BECs). Such phenomena can exist in homogeneous or periodic nonlinear systems. In optics, a spatial soliton formed in periodic nonlinear media (such as waveguide arrays) is often called a ''discrete soliton'' [2] if its propagation constant resides in the semi-infinite gap, or a ''gap soliton'' (GS) [3–5] if its propagation constant resides in a photonic band gap. A common belief is that lattice solitons must reside in a gap, but not inside Bloch bands. In fact, ''in-band'' solitons in periodic systems have never been demonstrated. A soliton whose propagation constant lies inside the continuous spectrum of radiation modes is also called an ''embedded soliton'' (ES) [6]. Although it has been shown theoretically that ESs could exist in homogeneous media [6] or in discrete (periodic) media with special nonlinearities [7], such solitons have never been observed in any physical systems.

In this Letter, we report the first experimental and theoretical demonstrations of in-band (embedded) lattice solitons. Such solitons are spatially localized in one transverse dimension, but extended as periodic wave trains in the other transverse dimension, propagating longitudinally without any change in shape. They are experimentally realized with a unique excitation of a quasi-one-dimensional (1D) stripe beam into a 2D optically induced photonic lattice. Different from all previously observed GSs [4,5], which typically bifurcate from the lowest or the highest edges of a Bloch band, the ESs established here bifurcate from the interior high-symmetry X points of the first band [denoted as X_1 in Fig. 1(a)], with their propagation constants remaining inside the 1st band. We also show that, at high powers, the propagation constants of ESs can move into the 1st band gap (between the 1st and 2nd Bloch bands), thus turning into GSs. This provides direct experimental evidence that GSs can bifurcate not only from the lowest or highest band edges but also from other locations inside a Bloch band. Our work could have direct impact on the study of nonlinear wave phenomena in other periodic systems such as condensed matter physics or BECs [8,9].

The experimental setup used for this work is similar to that we used earlier [10,11]. The lattice is induced in a 10 mm-long photorefractive SBN crystal by a spatially modulated partially coherent light beam (488 nm) sent through an amplitude mask. The mask is appropriately imaged onto the input face of the crystal, creating a periodic input intensity pattern [Fig. 1(b)] for optical induction of 2D lattices. With a negative bias voltage, a ''backbone'' waveguide lattice (23 μm spacing) is established as the crystal turns into a defocusing nonlinear medium [4,5]. The lattice beam is ordinarily polarized; thus, it experiences only a weak nonlinearity, while the probe beam is extraordinarily polarized and thus undergoes strong nonlinear propagation due to the anisotropic photorefractive nonlinearity. An incoherent background illumination is employed to fine-tune the nonlinearity [4,11]. To excite the X_1 points, the probe beam (cylindrically focused into a narrow stripe beam) is launched into the crystal collinearly with the lattice beam (i.e., without tilting angle), and the

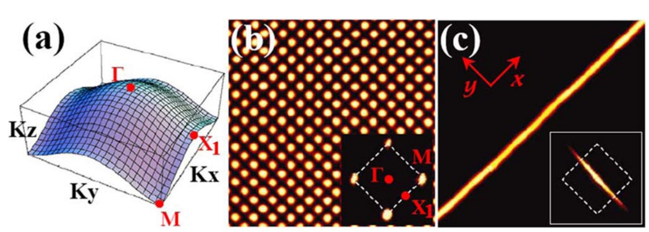

FIG. 1 (color online). (a) Structure of the 1st Bloch band for a square lattice with high-symmetry points marked by red dots. (b),(c) Lattice and probe beams at crystal input with corresponding k-space spectra shown in the insets. Dashed lines mark the 1st BZ.

stripe orientation is in parallel to one of the lattice principal axes [Fig. 1(c)]. Indeed, its spatial (k-space) power spectrum contains only wave numbers along the y axis, and it covers the two X points at the edge of the Brillouin zone (BZ) [4,5].

Under proper nonlinear conditions (i.e., a bias field of -1.5 kV/cm, lattice intensity of about 1, and probe intensity of 0.5 as normalized to background illumination), a soliton train is observed whose intensity profile is shown in Fig. 2(a). Interferograms between the soliton beam and a tilted plane wave reveal that this soliton train has a phase structure characteristic to Bloch modes at the X_1 points [12], as the adjacent stripes are out of phase with each other [Fig. 2(b)] while the peaks along the same stripe are all in phase [Fig. 2(c)]. This phase structure differs significantly from that of the fundamental soliton train in the semi-infinite gap bifurcating from the Γ point of the 1st band in focusing lattices [13], and from that of the GS train bifurcating from the M points of the 1st band in defocusing lattices [5]. In fact, the k-space spectrum of the soliton train in Fig. 2(d) shows that the spectrum is mostly located near two X points. Since these X points are *embedded* inside the 1st band, the soliton we obtained here is thus an ES. It is important to note that the distinctive spectrum in Fig. 2(d) is due to the nonlinear self-action of the stripe beam. For comparison, the spectrum of the same stripe beam propagating linearly (before the self-action takes place) through the lattice is also recorded in Fig. 2(e), which resembles the input spectrum in Fig. 1(c) but differs greatly from the soliton spectrum in Fig. 2(d). While experimentally it is difficult to monitor the beam propagation through the crystal, numerical results obtained with conditions corresponding to those of the experiment shows perfect agreement with results presented in Figs. 2(a)–2(e). Furthermore, simulations show that the ES can maintain its structure at propagation distances much longer than the crystal length [Fig. 2(f)].

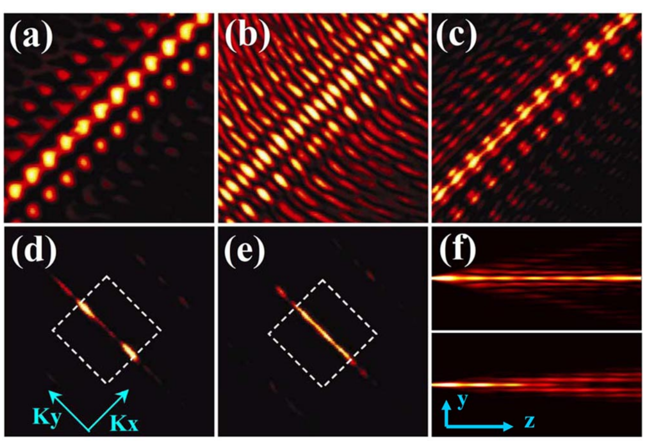

FIG. 2 (color online). Experimental observation of embedded soliton. (a)–(c) Output pattern of the soliton train and its interferograms with a plane wave tilted from two different directions. (d),(e) k-space spectrum for ES and for linear propagation, respectively. (f) Numerical simulation under nonlinear (top) and linear (bottom) propagation up to 30 mm.

The formation of in-band solitons is intriguing, as usually a soliton is not expected to exist inside the continuous spectrum [14]. This impels us to do further theoretical study, and to confirm what we observed is truly an ES in this periodic system. Our theoretical model is a (2 + 1)D NLS equation with a saturable defocusing nonlinearity and a periodic lattice potential [4,15]:

$$iU_z + U_{xx} + U_{yy} - \frac{E_0}{1 + I_L(x, y) + |U|^2} U = 0, \quad (1)$$

where U is the envelope function of the optical field, z is the propagation distance, (x, y) are the transverse coordinates, E_0 is the applied dc field, and $I_L(x, y) = I_0 \sin^2[(x + y)/\sqrt{2}] \sin^2[(x - y)/\sqrt{2}]$ is the lattice intensity pattern (with peak intensity I_0). All variables have been properly normalized [15]. For $I_0 = 1.5$ and $E_0 = -10$ (close to our experimental parameters), the lattice pattern and band gap structure are shown in Figs. 3(a) and 3(d). Soliton solutions in Eq. (1) are sought in the form of $U(x, y, z) = u(x, y) \times \exp(ik_z z)$, where k_z is the propagation constant (if k_z lies inside a Bloch band, i.e., the continuous spectrum, then the soliton is in-band or embedded). Using the modified squared-operator iteration method developed in [16], we do find a *family* of ES trains inside the 1st Bloch band bifurcating from the X_1 points. The power curve of these solitons is plotted in Fig. 3(d), where the power is defined over one period along the train direction. A typical solution of the ES train is shown in Figs. 3(b) and 3(c), which

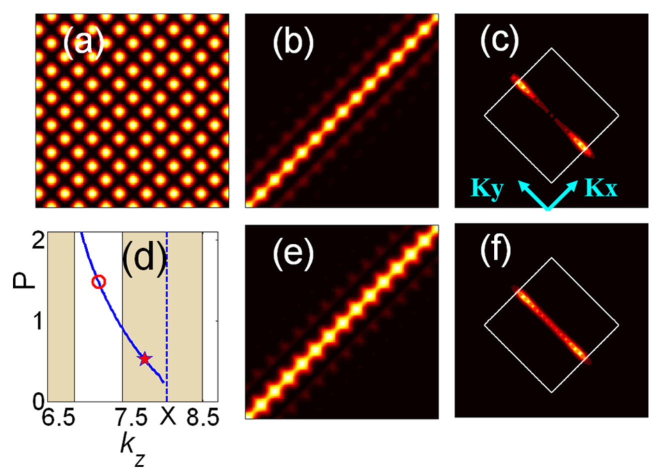

FIG. 3 (color online). Theoretical solutions for embedded and gap soliton trains in a square lattice of (a). Shown are the intensity and spectrum of an embedded (b),(c) and gap (e),(f) soliton. (d) The power verses propagation constant (k_z) diagram, where the red star (circle) in the 1st Bloch band (gap) marks the k_z location of the embedded (gap) soliton illustrated in the right panels. The dashed line in (d) corresponds to the location of the X point in the first band.

consists of several periodically modulated stripes. Close examination shows that the phase structure and spatial spectrum of this soliton solution are in agreement with that from the experiment of Fig. 2. More importantly, this solution exists with its propagation constant located *inside* the 1st Bloch band [marked by a red star inside the shaded 1st band in Fig. 3(d)] rather than in the 1st gap, revealing its nature of the ES.

The mechanism for formation of ESs merits further discussion. These solitons bifurcate from the interior high-symmetry X points in the 1st Bloch band, where the diffraction surface has a saddle shape; i.e., the diffraction coefficients have opposite signs along two orthogonal directions [Fig. 1(a)]. Specifically, the diffraction at the X_1 point marked in Fig. 1(a) is normal along the k_x direction but anomalous along the k_y direction. This saddle shape of the diffraction surface serves for two purposes. First, it makes the solitons existing near the saddle point to be embedded. Second, it dictates that these solitons must be localized along the y direction (where anomalous diffraction can be balanced by self-defocusing nonlinearity), but delocalized along the x direction. This existence mechanism is analogous to that for line solitons $U(x, y, t) = \sqrt{2}r\mathrm{sech}(ry)\exp(ir^2t)$ found in the $(2+1)$D NLS equation $iU_t - U_{xx} + U_{yy} + |U|^2U = 0$, where the dispersion surface also has a saddle shape. In addition, the ESs form a continuous family, similar to the above line solitons. We point out that line solitons have never been observed, as natural materials are not endowed with such saddle-shaped dispersion. Even in our induced photonic lattices, a circular or elliptical ES localized in both transverse dimensions would not exist near the X_1 points. The fact that ESs reside inside the continuous spectrum of the periodic system has important implications for their dynamical evolutions under perturbations. For instance, one of the key features of all ESs is the resonant continuous-wave radiation under perturbation [6,14].

Our analysis in Fig. 3(d) also shows that, when the power of the ES is high, its propagation constant can move into the photonic gap (between the 1st and 2nd bands) to form a ''true'' GS. A typical solution of the GS is presented in Fig. 3(e), whose intensity and phase structures are similar to those of the ES [Fig. 3(b)], but the location of the propagation constant is now in-gap rather than in-band. The spectrum of this GS [Fig. 3(f)] is also different from that of the ES [Fig. 3(c)], with two bright spots near X points merging towards the center, indicating that in the gap the soliton power is more concentrated in the central stripe. Unlike the conventional GSs [4,5], the GS train created here bifurcates from the interior X_1 points. This illustrates that GSs can bifurcate not only from the lowest or highest band edges but also from other locations inside a band. A similar feature has been discussed recently in the study of self-trapped gap waves in BECs [17].

Experimentally, it poses a challenge to identify the transition between an ES and a GS, since there is no phase transition between the two types of solitons, and the soliton existence curve is continuous from the band to the gap

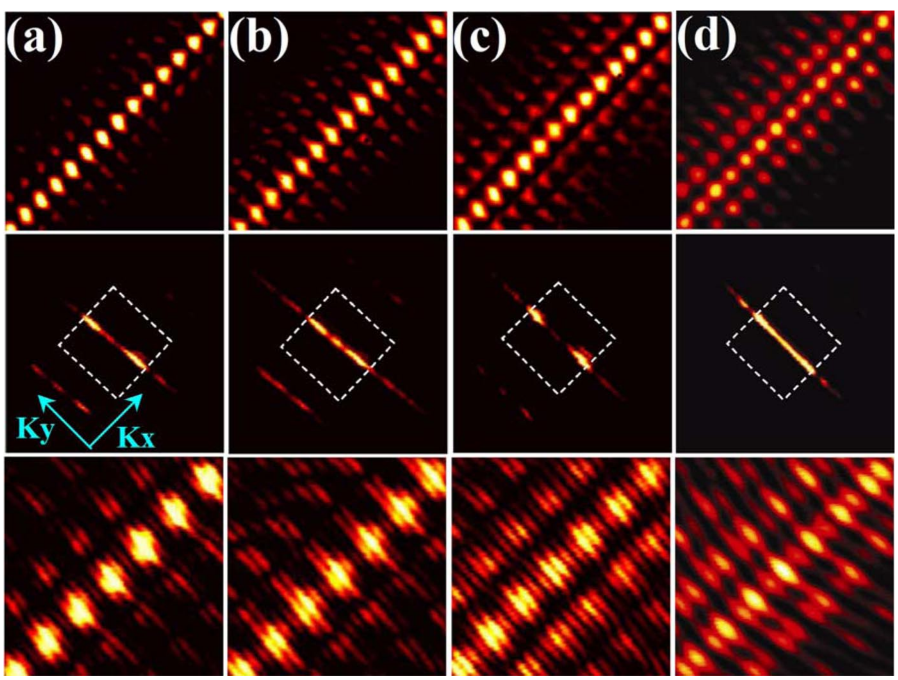

FIG. 4 (color online). Observation of transition between embedded and gap solitons. (a) An ES formed at low power, (b) transition to a GS at higher power, (c) restoration of an ES at reduced lattice potential, and (d) deterioration of the soliton when the lattice potential is too low (see text for details). From top to bottom are the output intensity patterns, spectra, and interferograms.

[Fig. 3(d)]. Nevertheless, we perform a series of experiments under different conditions in order to observe the subtle difference between an ES and a GS. An example from experimental results is presented in Fig. 4. First, with a low-power beam (about 0.5 probe-to-lattice intensity ratio), an ES is established [Fig. 4(a)] under conditions similar to those of Fig. 2. Second, the intensity ratio is increased to about 1.0 with all other conditions unchanged, then a new soliton state is achieved as shown in Fig. 4(b). While the intensity and phase structure appears to be similar, the change in the spectrum is clearly visible as the two bright spots tend to merge towards the center at the higher power. This experimental observation agrees well with the theoretical results of Fig. 3, indicating that an ES can move into the gap as its power is increased. Furthermore, after the GS train is formed, we decrease the lattice potential (by reducing the lattice intensity by a factor of $1/3$ while keeping the same probe-to-lattice intensity ratio), and we observe that the output of the soliton [Fig. 4(c)] again resembles an ES with a distinctive feature around the X points in the spectrum. This suggests that the reduced lattice potential (accompanied by narrowing of the gap and widening of the band) favors the formation of the ES when its power is not increased accordingly. Of course, if the lattice potential is too low to open a gap, the ES can no longer sustain as seen in Fig. 4(d), where the output spectrum becomes similar to that of the linear propagation in Fig. 2(e), and the interferogram no longer has an out-of-phase relation as shown in Figs. 4(a)–4(c). Numerical simulations under these conditions show similar behaviors. Despite this transition between in-band and in-gap solitons, we emphasize that the ESs established here are fundamentally different from all previously observed spatial GSs [4,5] or reduced-symmetry GSs [18]. In particular, the reduced-symmetry GSs arise from Bloch modes at the X points (band edge) of the second band, whereas the ESs arise from Bloch modes at the interior X points (subband edge) of the first band.

In summary, we have demonstrated a new type of spatial solitons, namely, in-band (or embedded) solitons. We have shown that an embedded soliton can move into a photonic band gap and turn into a gap soliton. These findings may have direct impact on the study of nonlinear waves and soliton phenomena in other branches of physics of periodic systems. For instance, we expect such solitons to exist also in BECs loaded in 2D optical lattice potential, now that nonlinear self-trapping of matter waves have been demonstrated in a number of experiments [9,17]. It would also be interesting to explore if similar phenomena can exist in other periodic systems such as condensed matter physics where gap solitons have also been demonstrated [8], and if such phenomena are related to persistent spin waves discussed for neutron-scattering experiments [19] or those electronics and molecular bound states embedded in the continuum [20], which have intrigued scientists for decades.

This work was supported by NSF, AFOSR, PRF, the 973 Program and PCSIRT.

[1] M. J. Ablowitz and H. Segur, *Solitons and the Inverse Scattering Transform* (SIAM, Philadelphia, 1985); Y. S. Kivshar and G. Agrawal, *Optical Solitons: From Fibers to Photonic Crystals* (Academic, San Diego, 2003).
[2] D. N. Christodoulides and R. I. Joseph, Opt. Lett. **13**, 794 (1988); H. S. Eisenberg *et al.*, Phys. Rev. Lett. **81**, 3383 (1998); D. N. Christodoulides, F. Lederer, and Y. Siberberg, Nature (London) **424**, 817 (2003).
[3] Y. S. Kivshar, Opt. Lett. **18**, 1147 (1993).
[4] J. W. Fleischer *et al.*, Phys. Rev. Lett. **90**, 023902 (2003); J. W. Fleischer *et al.*, Nature (London) **422**, 147 (2003); D. Mandelik *et al.*, Phys. Rev. Lett. **92**, 093904 (2004); D. N. Neshev *et al.*, *ibid.* **93**, 083905 (2004).
[5] C. Lou *et al.*, Phys. Rev. Lett. **98**, 213903 (2007); Z. Shi and J. Yang, Phys. Rev. E **75**, 061302 (2007).
[6] J. Yang *et al.*, Phys. Rev. Lett. **83**, 1958 (1999); J. Yang, *ibid.* **91**, 143903 (2003).
[7] K. Yagasaki *et al.*, Nonlinearity **18**, 2591 (2005).
[8] W. P. Su *et al.*, Phys. Rev. Lett. **42**, 1698 (1979); M. Aïn *et al.*, *ibid.* **78**, 1560 (1997).
[9] B. Eiermann *et al.*, Phys. Rev. Lett. **92**, 230401 (2004).
[10] Z. Chen and K. McCarthy, Opt. Lett. **27**, 2019 (2002).
[11] H. Martin *et al.*, Phys. Rev. Lett. **92**, 123902 (2004).
[12] A. A. Sukhorukov *et al.*, Phys. Rev. Lett. **92**, 093901 (2004); D. Träger *et al.*, Opt. Express **14**, 1913 (2006).
[13] Z. Chen *et al.*, Phys. Rev. Lett. **92**, 143902 (2004).
[14] J. P. Boyd, *Weakly Nonlocal Solitary Waves and Beyond-All-Orders Asymptotics* (Kluwer, Boston, 1998).
[15] N. K. Efremidis *et al.*, Phys. Rev. Lett. **91**, 213906 (2003); J. Yang, New J. Phys. **6**, 47 (2004).
[16] J. Yang and T. I. Lakoba, Stud. Appl. Math. **118**, 153 (2007).
[17] Th. Anker *et al.*, Phys. Rev. Lett. **94**, 020403 (2005); T. J. Alexander *et al.*, *ibid.* **96**, 040401 (2006).
[18] R. Fischer *et al.*, Phys. Rev. Lett. **96**, 023905 (2006).
[19] Y. J. Uemura *et al.*, Phys. Rev. Lett. **51**, 2322 (1983).
[20] L. S. Cederbaum *et al.*, Phys. Rev. Lett. **90**, 013001 (2003).